

Radical formation in polymer electrolyte fuel cell components as studied by ESR spectroscopy

Masahiro Kitazawa · Atsuko Y. Nosaka · Yoshio Nosaka

Received: 4 July 2007 / Revised: 20 November 2007 / Accepted: 27 November 2007 / Published online: 11 December 2007
© Springer Science+Business Media B.V. 2007

Abstract To clarify the deterioration mechanism for polymer electrolyte fuel cells, OH radical formation at the catalyst electrodes was investigated by ESR (electron spin resonance) spectroscopy using a flow cell with the catalyst electrodes. OH radicals produced from H_2O_2 were detected by a DMPO (5,5-dimethyl-1-pyrroline N-oxide) spin-trapping method for a Nafion-coated Pt/Carbon catalyst electrode under a high potential (0.85 V versus RHE) on supplying H_2 and under low potentials (lower than 0.40 V). When Pt–Ru catalysts were employed instead of Pt catalysts, the formation of OH radicals was barely detected. The results suggest the possibility of the formation of OH radicals by the oxidation of H_2O_2 at the oxidized Pt surface under a positive potential as well as the reduction of H_2O_2 at the clean Pt surface under a low potential.

Keywords Polymer electrolyte fuel cell · DMPO · Deterioration · ESR · Spin trapping · OH radical

1 Introduction

Polymer electrolyte fuel cells (PEFCs) have prospects as devices for clean and efficient energy conversion. A major concern for the practical use of PEFCs is durability. One of the most urgent technical problems is the prevention of membrane electrode assembly (MEA) deterioration during operation. An MEA consists of a cathode, an anode and a polymer electrolyte membrane (PEM) sandwiched between the two electrodes. MEA deterioration results from the

attack of reactive radical species formed from H_2O_2 at the MEA during operation. By means of a rotating ring-disk electrode technique, it was indicated that hydrogen peroxide (H_2O_2) could be formed through a two-electron reduction of O_2 on catalytic sites such as platinum [1, 2]. Inaba and co-workers reported that, in the presence of O_2 , a large amount of H_2O_2 was produced by the reduction of O_2 over Pt catalysts situated at a relatively negative potential. Therefore, if O_2 is cross-leaked during operation, H_2O_2 would be formed preferably on the anode side of the cell through the reduction of the cross-leaked O_2 . However, they reported that a significant amount of H_2O_2 was also produced from O_2 on highly dispersed Pt catalysts even at cathode potentials [2]. By employing thin Pt wires as working electrodes, the concentration of H_2O_2 at the proton exchange membrane was determined to be about 10 ppm [3]. Yano et al. have recently reported that the H_2O_2 yield is 0.6–1.0% of the overall oxygen reduction reaction at 0.7–0.8 V on Nafion-coated Pt/carbon-black. They indicated that the Nafion coating is a major factor in H_2O_2 formation on Pt catalysts by modifying the surface properties [4].

H_2O_2 released on the electrode catalysts was suggested to form OH radicals by reacting with contaminant metal ions such as Fe^{2+} [5]. Endoh et al. detected radicals in the catalyst layers of degraded MEAs. Though the experiments were carried out under low-humidified open-circuit conditions, they suggested that the radicals should be either $\bullet\text{OH}$ or hydroperoxyl radicals ($\bullet\text{O}_2\text{H}$) or both, generated by reaction with the carbon black [6]. Although they found radicals on the carbon, catalyst degradation is not usually the fatal factor in the degradation of MEA; rather the degradation of PEM is believed to be the most important factor. The formation of OH radicals to react with Nafion is considered a process causing the deterioration of PEM.

M. Kitazawa · A. Y. Nosaka · Y. Nosaka (✉)
Department of Chemistry, Nagaoka University of Technology,
Kamitomioka, Nagaoka 940-2188, Japan
e-mail: nosaka@nagaokaut.ac.jp

In the presence of Fe^{2+} , $\bullet\text{OH}$ would undoubtedly be formed from H_2O_2 in PEM. However, the nature and the amount of contaminant metal ions contained in the PEM are still unclear.

H_2O_2 is produced preferably at the anode as stated above [2], and F^- release at the anode side is larger than that at the cathode side when the PEM of the PEFC was degraded [7]. By mounting a running fuel cell [8] in the microwave cavity of an electron spin resonance (ESR) spectrometer, however, Roduner and co-workers demonstrated the formation of OH radicals at the cathode with a spin-trapping reagent, DMPO (5,5-dimethyl-1-pyrroline N-oxide) [9]. This report would still be debatable because the H_2O_2 formation and the F^- release in PEFC operations have been suggested as described above.

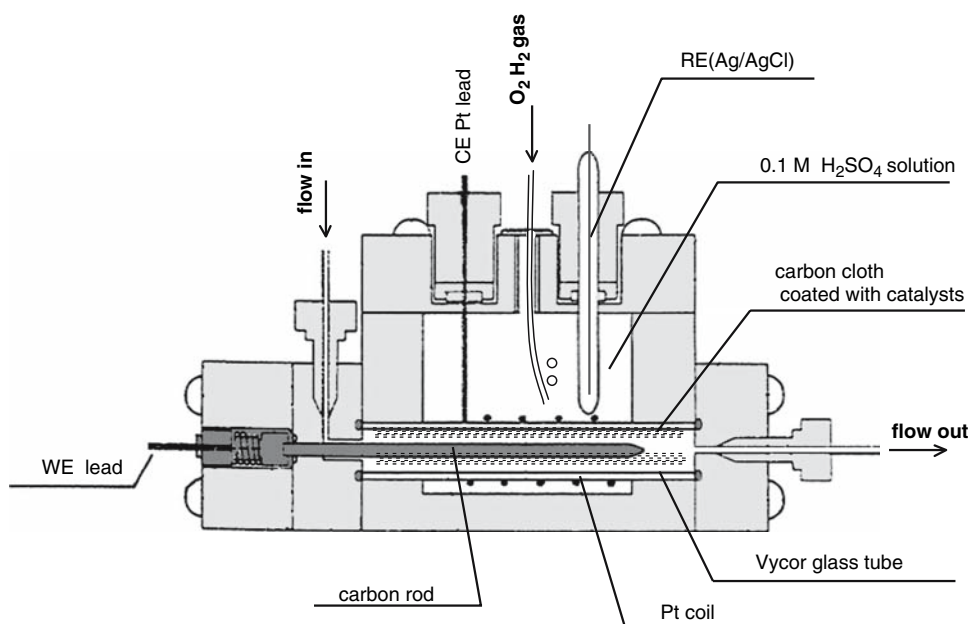
In the present study, to clarify the relationship between the polarization of the catalyst electrodes and the formation of OH radicals, we investigated the formation of $\bullet\text{OH}$ at polarized electrodes using ESR spectroscopy. Namely, a carbon cloth loaded with catalysts was used as an electrode in a flow cell, and OH radicals generated on potential application were measured by ESR spectroscopy with a spin-trapping reagent, DMPO. The effect of Ru alloying and the contaminant of H_2 gas were investigated as well as the effect of applied potential at Pt/C electrodes on the formation of OH radicals.

2 Experimental

Figure 1 shows the flow electrolysis cell used in the present study. A commercially available flow cell (HX-201, Hokuto

Denko Co., Ltd.) was modified. The original working electrode of a bunch of carbon fibers [10] was replaced by a rolled carbon cloth (5 cm \times 10 cm) on which catalyst powders were deposited. The deposition was performed by spraying a catalyst-Nafion slurry on a carbon cloth heated on a hot plate at 80 °C. The catalyst powders used were Pt/C at 45% loading (TEC10E50E, Tanaka Kikinzoku Kogyo) and Pt–Ru/C (Pt:Ru = 1:1.5 (mol)) loaded at 54% on C (TEC61E54, Tanaka Kikinzoku Kogyo). The catalyst/Nafion ratio of the slurry was 0.9 for Pt/C and 1.2 for Pt–Ru/C. The amount of the catalysts on the carbon cloth was 0.5 mg-Pt/cm² for both Pt/C and Pt–Ru/C. The carbon cloth was tightly fixed to a carbon rod (5 mm in diameter and 100 mm in length) with a Teflon string. The end of the rod was connected to a lead wire for potential application as a working electrode (WE). The rolled carbon cloth was placed in a Vycor glass tube (10 mm in outer diameter and 50 mm in length) to separate it from the Pt counter electrode (CE) coiled around the tube. The outside of the Vycor glass tube was filled with an electrolyte solution of 0.1 M H_2SO_4 . The solution was allowed to flow through inside the tube at a rate of 0.4 ml/min using a pump (Dual Pump 201, Flom Co., Ltd). To examine the effect of dissolved gas, O_2 or H_2 gas was introduced into the electrolyte solution from outside the Vycor glass tube with a fine Teflon tube. The potentiostat used was a Type PS-07 (Toho Technical Research), and the current was recorded with an X–Y recorder (F-35C, Riken Denshi). The potential applied with an Ag/AgCl reference electrode (HX-R5, Hokuto Denko) was converted into the RHE scale using the pH value of the electrolyte used (pH = 0.89). For example, 0.00 V versus Ag/AgCl was converted to 0.25 V versus RHE.

Fig. 1 Cross-sectional view of the flow electrolysis cell used



ESR measurements were performed with a JEOL JES-RE3X X-band spectrometer modified with a digital unit and a WIN-RAD operation system (RX, Radical Research Inc.). The flow from the electrolysis cell was introduced into a thin flat quartz cell ($0.3 \times 5 \times 50 \text{ mm}^3$) mounted in the cavity of the ESR spectrometer. ESR measurements were performed at a microwave power of 10 mW, a modulation field strength of 0.2 mT, a sweep width of 10 mT, a sweep time of 2 min, and a time response of 0.03 s, unless otherwise stated.

3 Results

3.1 Observation of OH radical adduct

To investigate the effect of the electrical potential of the catalysts on the radical formation, ESR measurements were performed under electrolysis in a flow cell. Figure 2a shows the ESR spectra observed at a rest potential (0.1 V versus RHE), and Fig. 2b shows those on potential application (0.85 V versus RHE) measured at intervals of 2 min. The small signals observed at the rest potential (A) were drastically enhanced under potential application (B). The four signals observed between 321 and 326 mT with a relative intensity of 1:2:2:1 in each spectrum were attributed to the DMPO-OH radical adduct based on a peak separation of 1.48 mT and a central g value of 2.006. The large signals on both sides in the spectrum are the standard signals of the Mn^{2+} marker in the ESR cavity. The relative amount of the radicals was estimated from the peak height of the second peak of the DMPO-OH signals divided by the peak height of the Mn^{2+} signal. By comparing the signal intensities with that of a stable radical (4-carboxy-2,2,6,6-tetramethylpiperidine-1-oxyl), one unit of the radical amount could be estimated to correspond to about 4 μM for the DMPO-OH adduct.

The relative heights of the second peak of the DMPO adduct signals recorded at four representative potentials are plotted as a function of the time in the flow electrolysis in Fig. 3. The noise level in Fig. 3 was about 0.2, judging from Fig. 2, which corresponds to 0.8 μM in the concentration of the DMPO-OH adduct.

3.2 Potential dependence of the $\bullet\text{OH}$ formation

In Fig. 4a and c, the concentrations of DMPO-OH radicals calculated from the averaged signal intensities for Pt-Ru/C and Pt/C electrodes are plotted as a function of the applied potential. In the bottom half in the figure, the currents observed during the ESR measurements are also plotted (Fig. 4b and d for Pt-Ru/C and Pt/C, respectively).

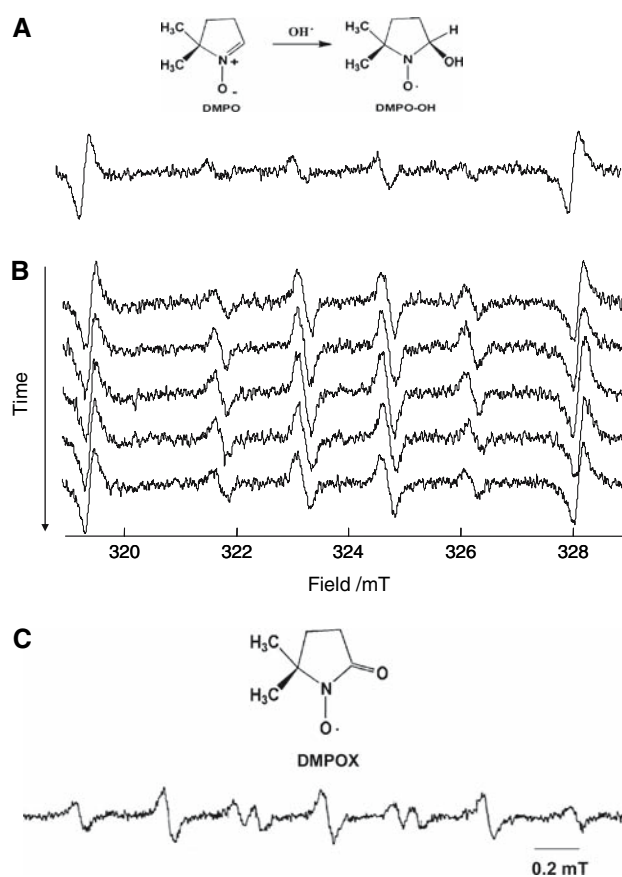


Fig. 2 ESR spectra measured with the applied potential of (a) 0.1, (b) 0.85, (c) 1.25 V (versus RHE) during electrolysis with a Pt/C catalyst electrode in 0.1 M H_2SO_4 solution containing 90 mM H_2O_2 and 10 mM DMPO. The sweep time was 2 min in the ESR measurements, and the modulation field strength, the sweep width, and the time constant were 0.2 mT, 10 mT, and 0.03 s for spectra (a, b) and 0.01 mT, 7 mT, and 0.1 s for spectrum (c), respectively. The large signals at both ends in (a, b) are the external reference signals of Mn^{2+}

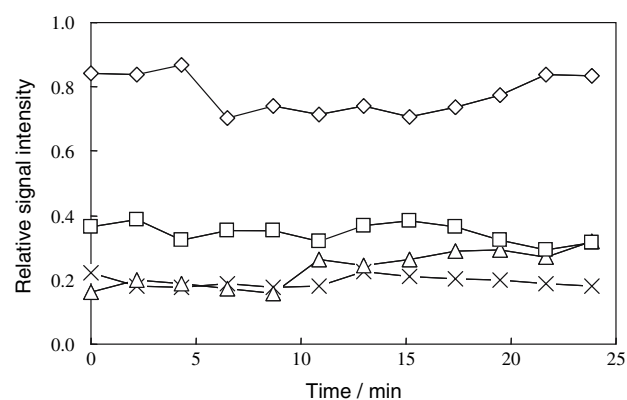
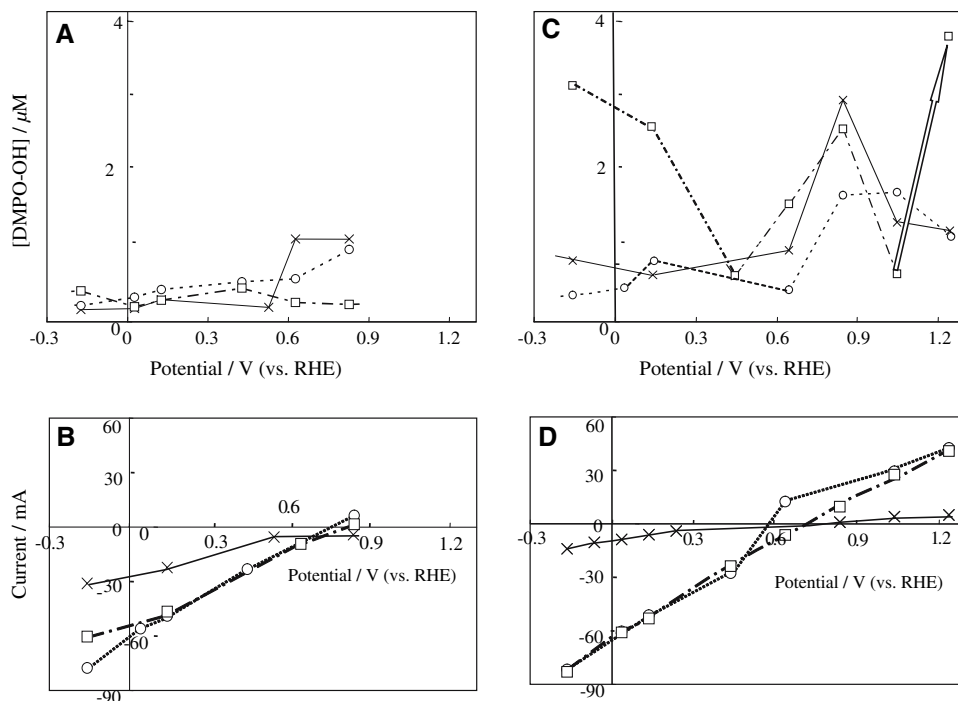


Fig. 3 Signal intensity of the second peak relative to Mn^{2+} signal in the ESR spectra of DMPO-OH adduct plotted as a function of time in the flow electrolysis under the potential of -0.25 (×), 0.65 (△), 0.85 (◇), and 1.05 (□) V (versus RHE)

Fig. 4 Concentration of DMPO-OH radical (a, c) and the current (b, d) under various potentials for 0.1 M H₂SO₄ solution containing 10 mM DMPO and 90 mM H₂O₂ (×), on supplying O₂ (○) and H₂ (□) gasses to the electrolyte solution. The electrodes were modified with Pt–Ru/C (a, b) and Pt/C (c, d) catalysts. The symbol indicated by the arrow shows the formation of another nitroxide radical, DMPOX

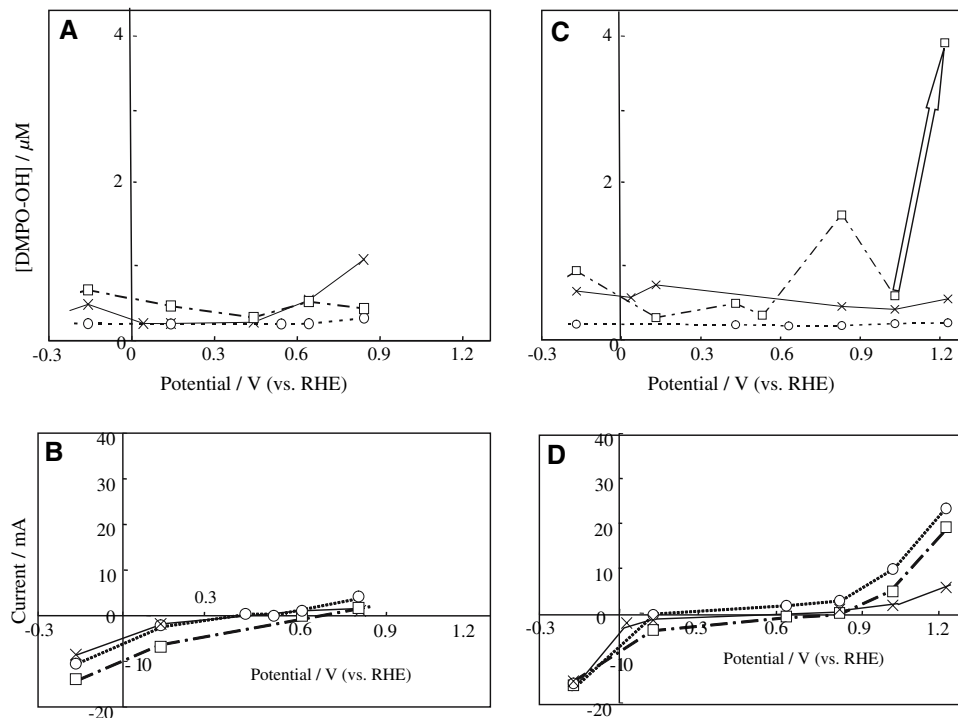


The measurements were performed in 0.1 M H₂SO₄ containing 90 mM H₂O₂ and 10 mM DMPO, without supplying gas (×), and saturated with O₂ (○) or H₂ (□). For comparison, similar measurements were performed in the electrolyte solution without adding H₂O₂ as shown in Fig. 5. The current shown in Fig. 5b and d did not alter drastically on saturation with H₂ or O₂. Because the gas

was supplied from outside the Vycor diaphragm, the dissolved gas may be insufficient to cover the working electrode in the flowing electrolyte.

In the absence of DMPO without gas supply, the same current as in Fig. 5d (×) was observed. No electrode reaction then occurs with DMPO, though the effect of DMPO on the surface reaction of H₂O₂ cannot be ruled out.

Fig. 5 Concentration of DMPO-OH radical (a, c) and the current (b, d) under various potentials for 0.1 M H₂SO₄ solution containing 10 mM DMPO (×), on supplying O₂ (○) and H₂ (□) gasses to the electrolyte solution. The electrodes were modified with Pt–Ru/C (a, b) and Pt/C (c, d) catalysts. The symbol indicated by the arrow shows the formation of another nitroxide radical, DMPOX



3.3 Formation of another radical

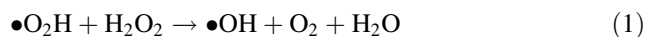
For Pt/C catalysts at 1.2 V versus RHE, the ESR signal was different from that of the DMPO-OH adduct. As was confirmed from the ESR spectrum (Fig. 2c) measured at high resolution (a low modulation field), the hyperfine coupling constants were estimated to be $a_N = 0.725$ mT and $a_H = 0.403$ mT, respectively, which agree well with those reported for DMPOX (5,5-dimethyl-2-oxopyrroline-1-oxyl) radicals [11]. As indicated by the arrows in Figs. 4c and 5c, DMPOX radicals replaced the DMPO-OH radicals only when H₂ gas was introduced. This observation indicates that the produced DMPO-OH radicals decomposed to some diamagnetic species which became DMPOX radicals with H₂ at this potential. This radical may be produced by the electrochemical oxidation of DMPO, though the oxidation process is not the same as that reported in the literature [11] where chlorine radicals are involved in the oxidation.

4 Discussion

4.1 Under high potential

Under a higher electrical potential of more than 0.5 V, for the Pt-Ru/C electrode, a small amount of •OH was observed without gas (×) and for the introduction of O₂ (○) but was not observed on supplying H₂ (□) as shown in Fig. 4a. On the other hand for the Pt/C electrode, as shown in Fig. 4c, under a high electrical potential at a polarization of 0.85 V (versus RHE), a significant amount of OH radicals was formed from H₂O₂ without supplying gas (×), and on supplying O₂ (○) or H₂ (□) gasses. Although slight, an anodic current was observed at this potential as indicated in Fig. 4d. These observations suggest that OH radicals should be produced at the cathode side rather than at the anode side, which is consistent with the report by Roduner and coworkers [9].

A possible explanation for the formation of •OH on the oxidation of H₂O₂ is that •O₂H is released through the oxidation of H₂O₂ followed by a homogeneous non-electrolytic reaction with H₂O₂ for radical transformation (1)



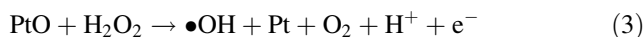
However, the oxidation of H₂O₂ in an acidic solution (2) takes place at a more positive potential [12] than that observed.



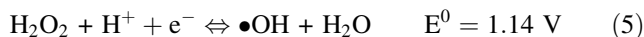
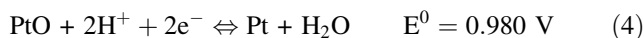
Thus the formation process of OH radicals via reactions (1) and (2) at 0.85 V cannot explain the present observation, though the formation of •O₂H in the oxygen

oxidation reaction on Pt electrodes has been suggested [13].

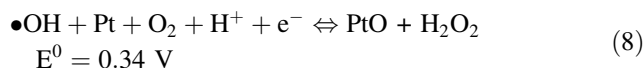
When the presence of PtO on Pt is assumed, the formation of OH radicals by oxidation of H₂O₂ can be expressed by the following reaction (3)



The standard redox potential for reaction (3) can be calculated with the following values reported for PtO, H₂O₂ and O₂ [12].



Taking into account Eqs. 4–7, the following relationship holds.



Because PtO is one of the reaction intermediates of oxygen reduction reactions, the oxidation of H₂O₂ with the reduction of PtO takes place to form OH radicals as expressed by reaction (3).

4.2 Under low potential

As shown in Fig. 4c, under a potential more negative than 0.4 V, the OH radical adduct was observed only when H₂ gas was introduced. A cathodic current of about –55 mA was observed at this potential; therefore, the •OH are formed by the reduction of H₂O₂ according to reaction (5).

Without H₂ gas, the •OH formed with cathodic current may be deactivated at the surface of Pt as suggested by Watanabe and co-workers [14]. On the other hand, at a potential of 0.85 V, the OH radicals formed may be more stable because of the positive polarization of the Pt catalyst. When Pt was alloyed with Ru, the formation of •OH at low potential was completely suppressed, even on supplying H₂, as shown in Fig. 4a. This suggests that Ru atoms in the Pt-Ru alloy have a role in accelerating the decomposition of H₂O₂ to produce H₂O and O₂.

4.3 Without H₂O₂

As shown in Fig. 5, in the absence of H₂O₂, no significant amount of OH radical adduct was observed for the Pt/C and Pt–Ru/C electrodes. Because the same current as in Fig. 5d was observed in the absence of DMPO, no electrode

reaction takes place for DMPO, though the possibility of the effect of DMPO on the surface reaction of H_2O_2 cannot be excluded completely. On supplying H_2 , a small amount of OH radicals was produced at 0.85 V versus RHE in the absence of H_2O_2 for the Pt/C electrode. The electrolyte was not completely deoxygenated; therefore, the contaminant O_2 might react with H_2 at this potential to produce H_2O_2 at the Pt/C electrode surface, leading to the formation of OH radicals.

5 Conclusions

By ESR spectroscopy using a flow cell with Pt/C and Pt–Ru/C catalysts, it was shown that, without H_2O_2 and electrolytic potential, OH radicals are not formed. At a high potential of 0.85 V (versus RHE), a significantly higher amount of OH radicals is produced from 0.3% H_2O_2 for the Pt/C electrode, in the presence of H_2 gas. On the other hand, at a low potential of less than 0.4 V, OH radicals are detected only on supplying H_2 to the Pt/C electrode.

Though H_2O_2 released on the catalysts probably forms OH radicals by reacting with contaminant metal ions such as Fe^{2+} [5], the present results indicate that, even in the absence of Fe^{2+} , OH radicals are formed from H_2O_2 at Pt/C at a positive potential and, to a lesser extent, at a negative potential. The suggested reaction mechanism for the formation of OH radicals at the cathode is the oxidation of H_2O_2 synchronized with the reduction of PtO to Pt in the oxygen reduction reaction.

Because the alloying of Ru reduced the formation of OH radicals even at low potentials, the deterioration of PEM may be prevented by alloying Pt electrodes with some

metal. OH radicals were formed at the cathode; therefore, modification of the cathode side with radical scavengers may be helpful in preventing PEM deterioration.

Acknowledgment We thank Mr. Satoru Watanabe and Ichiro Toyoda of Mitsubishi Heavy Industries for their support and helpful discussions. This work was supported by Research and Development of Polymer Electrolyte Fuel Cells from the New Energy and Industrial Technology Development Organization (NEDO), Japan.

References

1. Antoine O, Durand R (2000) *J Appl Electrochem* 30:839
2. Inaba M, Yamada H, Tokunaga J, Tasaka A (2004) *Electrochem Solid-State Lett* 7:A474
3. Liuz W, Zuckerbrod D (2005) *J Electrochem Soc* 152:A1165
4. Yano H, Higuchi E, Uchida H, Watanabe M (2006) *J Phys Chem B* 110:16544
5. Aoki M, Uchida H, Watanabe M (2006) *Electrochem Commun* 8:1509
6. Endoh E, Terazono S, Widjaja H, Takimoto Y (2004) *Electrochem Solid-State Lett* 7:A209
7. Inaba M, Kinumoto T, Kiriake M, Umebayashi R, Tasaka A, Ogumib Z (2006), *Electrochim Acta* 51:5746
8. Panchenko A, Dilger H, Möller E, Sixt T, Roduner E (2004) *J Power Sources* 127:325
9. Panchenko A, Dilger H, Kerres J, Hein M, Ullrich A, Kaz T, Roduner E (2004) *Phys Chem Chem Phys* 6:2891
10. Kusu F, Tamanouchi H, Sato T, Arai K, Takamura K, Sueoka T (1997) *Electrochemistry* 65:51
11. Brezova V, Valko M, Breza M, Morris H, Telser J, Dvoranova D, Kaiserova K, Varecka L, Mazur M, Leibfritz D (2003) *J Phys Chem B* 107:2415
12. Bard A J, Parsons R, Jordan J (eds) (1985) *Standard potentials in aqueous solution*. Marcel Dekker
13. Vogel WM, Baris JM (1977) *Electrochim Acta* 22:1259
14. Aoki M, Uchida H, Watanabe M (2005) *Electrochem Commun* 7:1434